

Angular Schmidt spectrum of entangled photons: derivation of an exact formula and experimental characterization for non-collinear phase matching

Girish Kulkarni, Lavanya Taneja, Shaurya Aarav, and Anand K. Jha*

Department of Physics, Indian Institute of Technology Kanpur, Kanpur, UP 208016, India

(Dated: June 18, 2022)

We derive an exact formula for the angular Schmidt spectrum of the orbital angular momentum (OAM)-entangled states produced by parametric down-conversion (PDC). We show that our formula yields true theoretical spectrum without any convergence issue as has been the case with the previously derived formulas. Furthermore, we use this formula to experimentally characterize the angular Schmidt spectrum for non-collinear PDC. We report the measurements of very broad angular Schmidt spectra corresponding to angular Schmidt numbers up to 233, which, to the best of our knowledge, is the highest number reported so far. Our studies can be very important for OAM-based quantum information applications.

The high-dimensional quantum information protocols offer many distinct advantages in terms of security [1–3], supersensitive measurements [4], violation of bipartite Bell’s inequality [5–9], enhancement of entanglement via concentration [10], and implementation of quantum coin-tossing protocol [11]. It has now been shown that the orbital angular momentum (OAM) of a photon provides a high-dimensional basis [12–14]. As a consequence, the OAM-entangled states of signal and idler photons produced by parametric down-conversion (PDC) have become a natural choice for high-dimensional quantum information applications. More specifically, there have been intense research efforts, both theoretically [15–21] and experimentally [22–28], for the precise characterization of high-dimensional OAM-entangled states produced by PDC. Although to completely characterize a general quantum state one requires full state tomography, an OAM-entangled pure quantum state can be characterized by measuring just the angular Schmidt spectrum [15, 16, 26], which is defined as the probability S_l of signal and idler photons getting detected in coincidence with OAM values $l\hbar$ and $-l\hbar$, respectively. The characterization of angular Schmidt spectra has been a very challenging problem. While on the experimental side the major challenge has been to find an efficient method for measuring the true spectrum, the main challenge on the theoretical side has been to develop a formalism, in the form of a formula, for the accurate estimation of the spectrum for various phase matching conditions.

Several experimental techniques have been developed for measuring the angular Schmidt spectrum. The first set of techniques were based on using projective measurements [22–25, 27]. However, these techniques are not very inefficient because the required number of measurements scales with the size of the input spectrum and also because these techniques measure only the projected spectrum instead of the true spectrum. The second set of techniques were based on measuring the angular coherence function in a two-photon interference experiment [19, 26]. Although these techniques do measure true Schmidt spectra, they require a series of coincidence mea-

surements and suffers from either the strict interferometric stability requirements [26] or too much loss [19]. More recently, an interferometric technique has been demonstrated [28] that can not only measure the true angular Schmidt spectrum but can also do so in a single-shot noise-insensitive manner without requiring coincidence detection. On the theoretical side, Torres *et al.* have derived a formula for calculating the spectrum for collinear phase matching [16]. However, this formula involves infinite summations and although the authors show that the summation converges for certain parameter sets, the convergence is not explicitly proved for an arbitrary set of parameters. More recent efforts have derived similar formulas incorporating non-collinear phase matching and more general PDC settings [17, 18, 21]. However, these formulas also involve infinite summations and thus suffer from the same convergence issue. Thus, although the past efforts have been able to greatly overcome the experimental challenges in measuring the true angular Schmidt spectrum, the theoretical challenges in the correct and efficient estimation of angular Schmidt spectrum are still there to be fully resolved.

In this letter, we derive an exact formula for calculating the angular Schmidt spectrum. Our formula does not involve infinite summations and thus have no convergence issue and is applicable to a very general set of phase-matching conditions and geometries. Using this formula, along with the single-shot technique developed in Ref. [28], we report experimental characterization of angular Schmidt spectrum for non-collinear phase matching.

Let us consider the situation shown in Fig. 1. A Gaussian pump beam undergoes parametric down-conversion inside a nonlinear crystal of thickness L . We work out the theory for Type-I phase matching with the pump photon being extra-ordinary polarized and the signal and idler photons being ordinary polarized. The beam waist of the pump field is located at a distance d behind the front surface of the crystal. The crystal is rotated by an angle α with respect to the incident direction of the pump beam, and the z -axis is defined to be the direction of the refracted pump beam inside the crystal. The angles that

the optic axes of the unrotated and rotated crystals make with the pump beam inside the crystal are denoted by θ_{p0} and θ_p , respectively. From Fig. 1, we find that

$$\theta_p = \theta_{p0} + \sin^{-1}(\sin \alpha / \eta_p), \quad (1)$$

where η_p is the refractive index of the extraordinary pump photons. By changing θ_p , one can go from collinear to non-collinear down-conversion.

Our first aim is to derive a formula for the angular Schmidt spectrum of OAM-entangled states. The state $|\psi_2\rangle$ of the down-converted signal and idler photons at the exit surface inside the crystal is written in the transverse-momentum basis as [16, 29, 30]:

$$|\psi_2\rangle = \iint_{-\infty}^{\infty} \Phi(\mathbf{q}_s, \mathbf{q}_i) |\mathbf{q}_s\rangle_s |\mathbf{q}_i\rangle_i d\mathbf{q}_s d\mathbf{q}_i, \quad (2)$$

$$\text{where } \Phi(\mathbf{q}_s, \mathbf{q}_i) = AV(\mathbf{q}_s + \mathbf{q}_i) e^{ik_{pz}d} \times \text{sinc}\left(\frac{\Delta k_z L}{2}\right) \exp\left(i\frac{\Delta k_z L}{2}\right). \quad (3)$$

Here, p, s, i stands for signal, idler and pump, respectively, A is a constant and $\text{sinc}(x) \equiv \sin x/x$. We have used $\mathbf{k}_j \equiv (k_{jx}, k_{jy}, k_{jz}) \equiv (q_{jx}, q_{jy}, k_{jz}) \equiv (\mathbf{q}_j, k_{jz})$, with $j = p, s, i$, and $\Delta k_z = k_{pz} - k_{sz} - k_{iz}$. The quasi-monochromaticity condition is assumed for each of the signal, idler and pump photons with their central wavelengths given by λ_s, λ_i , and λ_p , respectively. In addition, the transverse size of the crystal is taken to be much larger compared to the spot-size of the pump beam, ensuring $\mathbf{q}_p = \mathbf{q}_s + \mathbf{q}_i$. The quantity $V(\mathbf{q}_s + \mathbf{q}_i) e^{ik_{pz}d}$ is the spectral amplitude of the pump field at $z = 0$, wherein

$$V(\mathbf{q}_s + \mathbf{q}_i) = \frac{w_p}{\sqrt{2\pi}} \exp\left(-\frac{|\mathbf{q}_s + \mathbf{q}_i|^2 w_p^2}{4}\right) \quad (4)$$

is the spectral amplitude of the pump field at $z = 0$ with w_p being the width of the pump beam-waist. We take the expressions for k_{jz} from Ref. [30]:

$$k_{sz} = \sqrt{(2\pi n_{so}/\lambda_s)^2 - |\mathbf{q}_s|^2}, \quad k_{iz} = \sqrt{(2\pi n_{io}/\lambda_i)^2 - |\mathbf{q}_i|^2}, \\ \text{and } k_{pz} = \alpha_p q_{px} + \sqrt{(2\pi \eta_p/\lambda_p)^2 - \beta_p^2 q_{px}^2 - \gamma_p^2 q_{py}^2}, \quad (5)$$

where

$$\eta_p = n_{pe} \gamma_p, \quad \gamma_p = n_{po} / \sqrt{n_{po}^2 \sin^2 \theta_p + n_{pe}^2 \cos^2 \theta_p}, \\ \alpha_p = (n_{po}^2 - n_{pe}^2) \sin \theta_p \cos \theta_p / (n_{po}^2 \sin^2 \theta_p + n_{pe}^2 \cos^2 \theta_p), \\ \text{and } \beta_p = n_{po} n_{pe} / (n_{po}^2 \sin^2 \theta_p + n_{pe}^2 \cos^2 \theta_p). \quad (6)$$

Here n_{so} denotes the ordinary refractive index of the signal photon at wavelength λ_s , etc. We now write the state $|\psi_2\rangle$ in the Laguerre-Gaussian (LG) basis as [16–19]

$$|\psi_2\rangle = \sum_l \sum_{p_s} \sum_{p_i} C_{l,p_s,p_i} |l, p_s\rangle_s |l, p_i\rangle_i, \quad (7)$$

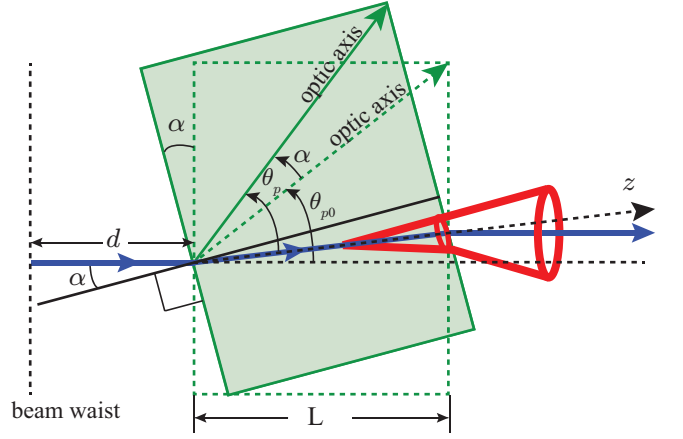


FIG. 1: (color online) Schematic of phase matching in PDC.

where $|l, p_s\rangle_s$ represents the state of the signal photon in the Laguerre-Gaussian mode defined by indices l and p_s , etc [12, 16, 17]. In writing this state, we have assumed OAM conservation in PDC, that is, $l_p = l_s + l_i$, which for a Gaussian pump beam with $l_p = 0$ implies $l_s = -l_i = l$ [22]. Using Eqs. (2) and (7), we write the coefficients C_{l,p_s,p_i} as

$$C_{l,p_s,p_i} = \iint \Phi(\mathbf{q}_s, \mathbf{q}_i) LG_{p_s}^{*l}(\mathbf{q}_s) LG_{p_i}^{*-l}(\mathbf{q}_i) d\mathbf{q}_s d\mathbf{q}_i. \quad (8)$$

Here $LG_{p_s}^l(\mathbf{q}_s) = \langle \mathbf{q}_s | l, p_s \rangle$ is the momentum-basis representation of state $|l, p_s\rangle$ [16, 17]. Moving to the cylindrical coordinates, we write C_{l,p_s,p_i} as

$$C_{l,p_s,p_i} = \iint_0^\infty \iint_{-\pi}^\pi \Phi(\rho_s, \rho_i, \phi_s, \phi_i) \times LG_{p_s}^{*l}(\rho_s, \phi_s) LG_{p_i}^{*-l}(\rho_i, \phi_i) \rho_s \rho_i d\rho_s d\rho_i d\phi_s d\phi_i, \quad (9)$$

where $\mathbf{q}_s \equiv (q_{sx}, q_{sy}) = (\rho_s \cos \phi_s, \rho_s \sin \phi_s)$, $\mathbf{q}_i \equiv (q_{ix}, q_{iy}) = (\rho_i \cos \phi_i, \rho_i \sin \phi_i)$, $d\mathbf{q}_s = \rho_s d\rho_s d\phi_s$, and $d\mathbf{q}_i = \rho_i d\rho_i d\phi_i$. The state $|\psi_2\rangle$ in Eq. 7 is in general an OAM-entangled state, and its angular Schmidt spectrum S_l is the probability that the signal and idler photons have OAM $l\hbar$ and $-l\hbar$, respectively. The angular Schmidt spectrum is defined as $S_l \equiv \sum_{p_s} \sum_{p_i} |C_{l,p_s,p_i}|^2$, and using Eq. (9) and the relation: $LG_p^l(\rho, \phi) = LG_p^l(\rho) e^{il\phi}$, we write it as

$$S_l = \iiint \iiint_0^\infty \iiint_{-\pi}^\pi \Phi(\rho_s, \rho_i, \phi_s, \phi_i) \Phi^*(\rho'_s, \rho'_i, \phi'_s, \phi'_i) \times \sum_{p_s=0}^\infty LG_{p_s}^{*l}(\rho_s) LG_{p_s}^l(\rho'_s) \sum_{p_i=0}^\infty LG_{p_i}^{*-l}(\rho_i) LG_{p_i}^{-l}(\rho'_i) \times e^{il(\phi_s - \phi_i)} e^{-il(\phi'_s - \phi'_i)} \times \rho_s \rho_i \rho'_s \rho'_i d\rho_s d\rho_i d\rho'_s d\rho'_i d\phi_s d\phi_i d\phi'_s d\phi'_i. \quad (10)$$

Next, using the identity $\sum_{p=0}^\infty LG_p^l(\rho) LG_p^{*l}(\rho') =$

$(1/\pi)\delta(\rho^2 - \rho'^2)$ over the indices p_s and p_i , we get

$$S_l = \iiint_0^\infty \iiint_{-\pi}^\pi \Phi(\rho_s, \rho_i, \phi_s, \phi_i) \Phi^*(\rho'_s, \rho'_i, \phi'_s, \phi'_i) \times \frac{1}{\pi^2} \delta(\rho_s^2 - \rho'^2_s) \delta(\rho_i^2 - \rho'^2_i) e^{il(\phi_s - \phi_i)} e^{-il(\phi'_s - \phi'_i)} \times \rho_s \rho_i \rho'_s \rho'_i d\rho_s d\rho_i d\rho'_s d\rho'_i d\phi_s d\phi_i d\phi'_s d\phi'_i \quad (11)$$

The above integral can be evaluated to yield:

$$S_l = \frac{1}{4\pi^2} \int_0^\infty \left| \int_{-\pi}^\pi \Phi(\rho_s, \rho_i, \phi_s, \phi_i) e^{il(\phi_s - \phi_i)} d\phi_s d\phi_i \right|^2 \times \rho_s \rho_i d\rho_s d\rho_i \quad (12)$$

Equation (12) is the main theoretical result of this letter, which shows that the angular Schmidt spectrum S_l can be computed directly as a four-dimensional integral by substituting from Eqs. (3) through (6). The formula in Eq. (12) does not have any infinite summation and therefore it does not suffer from the convergence issue that all the previously derived formulas [16–18, 21] suffer from. We note that the formula in Eq. (12) represents angular Schmidt spectrum just inside the nonlinear crystal. Nevertheless, in situations in which α is of the order of only a few degrees, the angular Schmidt spectrum inside and outside the crystal can be taken to be the same.

Next, we use Eq. (12) for experimentally characterizing the angular Schmidt spectrum for non-collinear phase matching conditions. We follow the experimental technique of Ref. [28], in which it was experimentally demonstrated that the angular Schmidt spectrum of OAM-entangled states can be measured by measuring the OAM spectrum of individual entangled photons without requiring coincidence detections [19]. Figure 2 shows our experimental setup for measuring the OAM spectrum of individual entangled photons. Following Ref. [28], we first define the measured OAM spectrum as

$$\bar{S}_l \equiv \int_{-\pi}^\pi \Delta \bar{I}_{\text{out}}(\phi) e^{i2l\phi} d\phi, \quad (13)$$

where δ denotes the overall phase difference between the two arms of the interferometer and where $\Delta \bar{I}_{\text{out}}(\phi) = \bar{I}_{\text{out}}^{\delta_c}(\phi) - \bar{I}_{\text{out}}^{\delta_d}(\phi)$ is the difference in the azimuthal intensities $\bar{I}_{\text{out}}^{\delta_c}(\phi)$ and $\bar{I}_{\text{out}}^{\delta_d}(\phi)$ of the two output interferograms recorded at $\delta = \delta_c$ and $\delta = \delta_d$, respectively. In situations in which the noises in the two interferograms are the same, it has been shown that $\bar{S}_l \propto S_l$, that is, the normalized measured OAM-spectrum \bar{S}_l is same as the normalized theoretical OAM-spectrum S_l , which is indeed the normalized angular Schmidt spectrum [19, 28]. Thus, without having to know the exact values of δ_c and δ_d or the other experimental parameters, the normalized angular Schmidt spectrum can be measured by recording just two output interferograms.

In the setup of Fig. 2, an ultraviolet continuous-beam pump laser (100 mW) of wavelength $\lambda_p = 405$ nm and

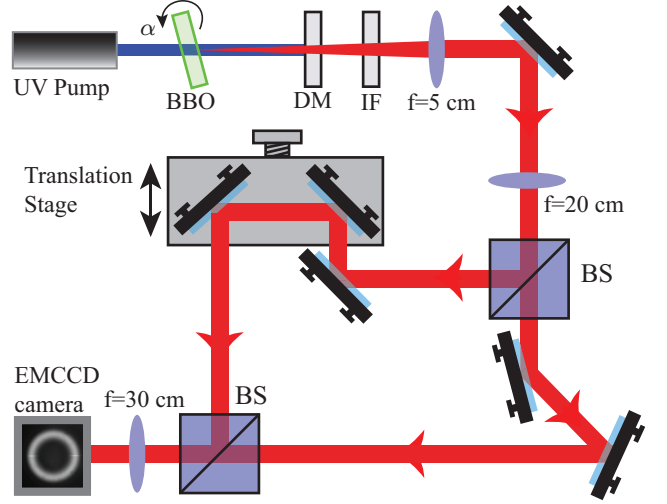


FIG. 2: (color online) Experimental setup for measuring the angular Schmidt spectrum. BBO is β -Barium Borate crystal; DM is a Dichroic mirror that reflects back the pump photon; IF is interference filter with 10 nm wavelength-bandwidth; and BS is beam splitter.

beam-waist width $w_p = 370 \mu\text{m}$ was used to produce type-I PDC inside a β -barium borate (BBO) crystal. The crystal was mounted on a goniometer which was rotated in steps of 0.04 degrees in order to change α and thereby θ_p . For a given setting of crystal and pump parameters, output interferograms were recorded for two values of δ , namely δ_c and δ_d , which differed by about half a wavelength and were introduced by displacing the automated translation stage by 200 nm after recording the first interferogram. The recording of the interferograms was done using an Andor Ixon Ultra EMCCD camera (512×512 pixels) with an acquisition time of 16 seconds. The lens combination in the setup was chosen such that the collection angle of the detection system was sufficiently larger compared to the emission cone angle of PDC. The azimuthal intensities $\bar{I}_{\text{out}}^{\delta_c}(\phi)$ and $\bar{I}_{\text{out}}^{\delta_d}(\phi)$ were obtained by first precisely positioning a very narrow angular region-of-interest (ROI) at angle ϕ in the interferogram image and then integrating the intensity within the ROI up to a sufficiently-large radius [28]. To reduce pixelation-related noise, the interferograms were scaled up in size by a factor of ten using a bicubic interpolation method. From a given pair of $\bar{I}_{\text{out}}^{\delta_c}(\phi)$ and $\bar{I}_{\text{out}}^{\delta_d}(\phi)$, $\Delta \bar{I}_{\text{out}}(\phi)$ was obtained and the angular Schmidt spectrum was then estimated using Eq. (13). In our experiments, $\lambda_s = \lambda_i = 810$ nm, $\lambda_p = 405$ nm, and $L = 2$ mm. We have used the following refractive index values taken from Ref. [31]: $n_{p_o} = 1.6923$, $n_{p_e} = 1.5680$ and $n_{s_o} = n_{i_o} = 1.6611$.

Figures 3 and 4 show our experimental and theoretical results. In Fig. 3, we have shown the details of our measurements for three values of θ_p . For each θ_p , we have plotted the measured output interferograms at $\delta = \delta_c$ and $\delta = \delta_d$, the difference azimuthal intensity $\Delta \bar{I}(\phi)$

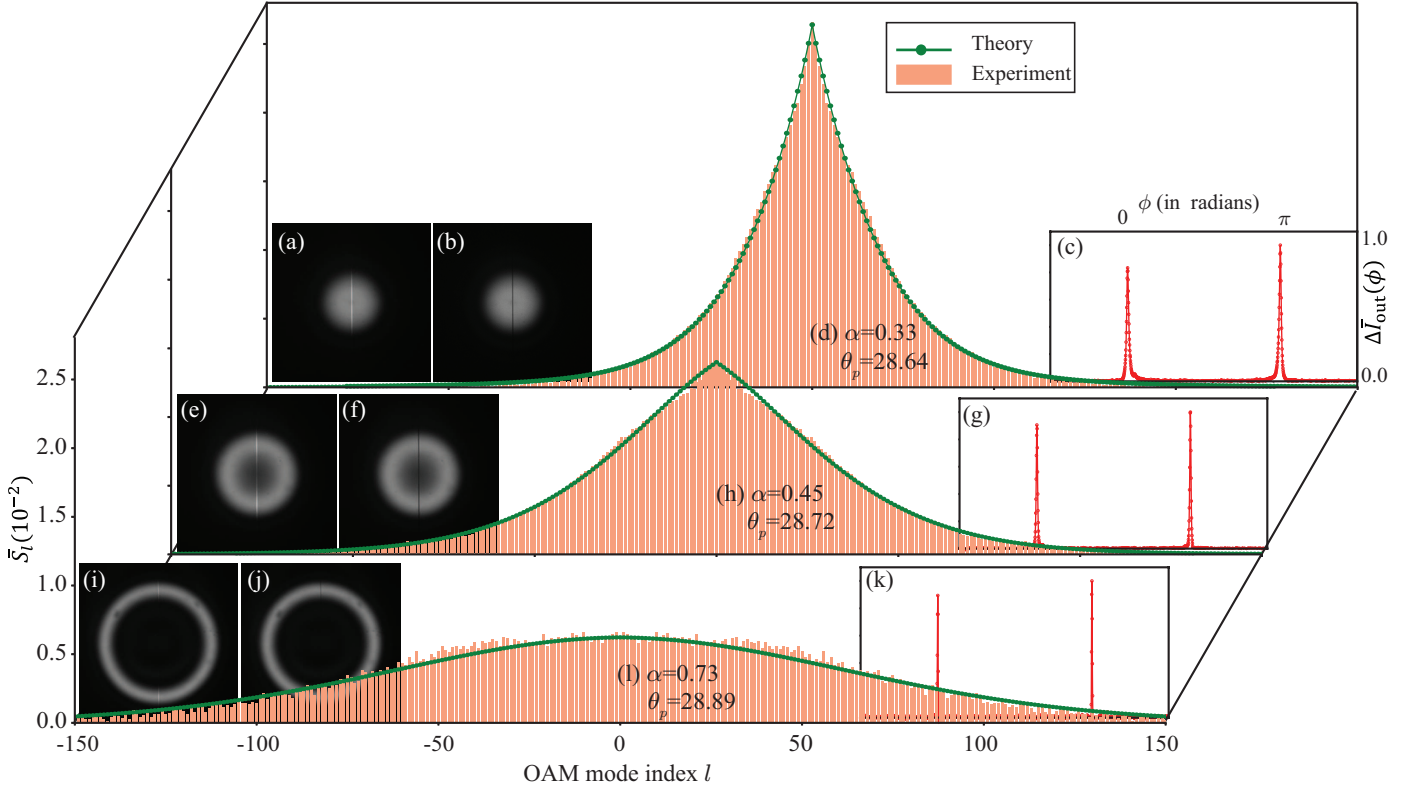


FIG. 3: (color online) (a), (b) The measured output interferograms at $\delta = \delta_c$ and $\delta = \delta_d$, respectively, (c) the difference $\Delta \bar{I}(\phi)$ in the azimuthal intensities of the two inteferograms, (d) The normalized measured spectrum as computed using Eq. (13) and the normalized theoretical spectrum as calculated using Eq. (12), for $\alpha = 0.33$ and $\theta_p = 28.64$. (e), (f), (g), (h) are the corresponding plots for $\alpha = 0.45$ and $\theta_p = 28.72$. (i), (j), (k), (l) are the corresponding plots for $\alpha = 0.73$ and $\theta_p = 28.89$.

along with the normalized spectrum as computed using Eq. (13) and the normalized theoretical spectrum as calculated using Eq. (12). The angular Schmidt number was calculated using the formula $K_a = 1 / (\sum_l \bar{S}_l^2)$. The experimentally measured angular Schmidt number along with the theoretical predictions at various θ_p values have been plotted in Fig. 4. We note that for our theoretical plots, θ_{p0} was the only fitting parameter, and once it was chosen, the subsequent θ_p values were calculated simply by substituting the rotation angle α in Eq. (1). We find that in general the angular Schmidt spectrum becomes broader with increasing non-collinearity. We measured very broad angular Schmidt spectra with the corresponding Schmidt numbers going as high as 233, which to the best of our knowledge is the highest ever reported angular Schmidt number.

We find excellent agreement between the theory and experiment, except for extremely non-collinear conditions, in which case the experimentally measured Schmidt numbers are slightly lower than the theoretically predictions. The main reason for this discrepancy is the limited resolution of our EMCCD camera. As described above, in order to generate the azimuthal intensity plots, we use narrow angular region of interest (ROI), the minimum possible size of which is fixed by the pixel size of

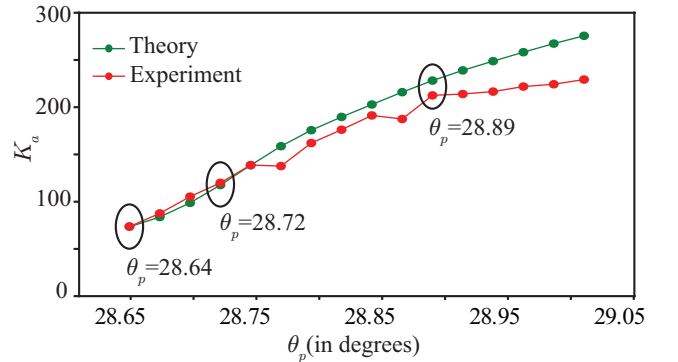


FIG. 4: (color online) Experimentally measured and theoretically estimated angular Schmidt number K_a as a function of θ_p . The details of angular Schmidt spectrum measurements corresponding to the three θ_p values indicated on the figure have been presented in Fig. 3.

the EMCCD camera. In the case of non-collinear down-conversion, the intensities in the interferograms are concentrated at some radii away from the center and therefore the corresponding $\Delta \bar{I}_{out}(\phi)$ plots gets generated with lesser angular resolution and thus estimated to be wider than their actual widths. This results in a slightly lower

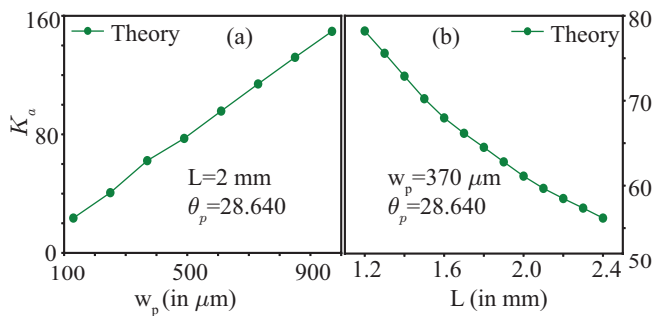


FIG. 5: (color online) (a) Theoretical dependence of the angular Schmidt number on the width of the pump beam waist w_p . (b) Theoretical dependence of the angular Schmidt number K_a on crystal thickness L .

estimate of the Schmidt numbers.

Finally, we use Eq. (12) for studying how w_p and L affect the angular Schmidt number K_a . Figure 5(a) shows the theoretical dependence of K_a on w_p for $L = 2 \text{ mm}$ and $\theta_p = 28.64$ degrees. Figure 5(b) shows the theoretical dependence of K_a on L for $w_p = 370 \mu\text{m}$ and $\theta_p = 28.64$ degrees. We find that the angular Schmidt number increase as a function of the width of beam waist w_p while it decreases as a function of the crystal thickness L .

In summary, we have derived in this letter an exact formula for the angular Schmidt spectrum of OAM-entangled photons produced by PDC. We have shown that our formula yields true theoretical spectrum without any convergence issue as has been the case with the previously derived formulas. Furthermore, we have used our theoretical formulation to experimentally characterize the angular Schmidt spectrum for non-collinear phase matching in PDC. The results reported in this letter provides theoretical and experiemtnal tools for efficient characterization of pure OAM-entangled state and can thus have important implication for high-dimensional quantum information applications.

We acknowledge financial support through an initiation grant no. IITK /PHY /20130008 from Indian Institute of Technology (IIT) Kanpur, India and through the research grant no. EMR/2015/001931 from the Science and Engineering Research Board (SERB), Department of Science and Technology, Government of India.

* Electronic address: akjha9@gmail.com

- [1] V. Karimipour, A. Bahraminasab, and S. Bagherinezhad, Phys. Rev. A **65**, 052331 (2002).
- [2] N. J. Cerf, M. Bourennane, A. Karlsson, and N. Gisin, Phys. Rev. Lett. **88**, 127902 (2002).
- [3] G. M. Nikolopoulos, K. S. Ranade, and G. Alber, Phys. Rev. A **73**, 032325 (2006).

- [4] A. K. Jha, G. S. Agarwal, and R. W. Boyd, Phys. Rev. A **83**, 053829 (2011).
- [5] D. Collins, N. Gisin, N. Linden, S. Massar, and S. Popescu, Phys. Rev. Lett. **88**, 040404 (2002).
- [6] J. Leach, B. Jack, J. Romero, M. Ritsch-Marte, R. W. Boyd, A. K. Jha, S. M. Barnett, S. Franke-Arnold, and M. J. Padgett, Opt. Express **17**, 8287 (2009).
- [7] A. Vaziri, G. Weihs, and A. Zeilinger, Phys. Rev. Lett. **89**, 240401 (2002).
- [8] D. Kaszlikowski, P. Gnaniński, M. Żukowski, W. Miklaszewski, and A. Zeilinger, Phys. Rev. Lett. **85**, 4418 (2000).
- [9] T. Vértesi, S. Pironio, and N. Brunner, Phys. Rev. Lett. **104**, 060401 (2010).
- [10] A. Vaziri, J.-W. Pan, T. Jennewein, G. Weihs, and A. Zeilinger, Phys. Rev. Lett. **91**, 227902 (2003).
- [11] G. Molina-Terriza, A. Vaziri, R. Ursin, and A. Zeilinger, Phys. Rev. Lett. **94**, 040501 (2005).
- [12] L. Allen, M. W. Beijersbergen, R. J. C. Spreeuw, and J. P. Woerdman, Phys. Rev. A **45**, 8185 (1992).
- [13] S. M. Barnett and D. T. Pegg, Phys. Rev. A **41**, 3427 (1990).
- [14] E. Yao, S. Franke-Arnold, J. Courtial, S. Barnett, and M. Padgett, Opt. Express **14**, 9071 (2006).
- [15] C. K. Law and J. H. Eberly, Phys. Rev. Lett. **92**, 127903 (2004).
- [16] J. P. Torres, A. Alexandrescu, and L. Torner, Phys. Rev. A **68**, 050301 (2003).
- [17] F. M. Miatto, A. M. Yao, and S. M. Barnett, Phys. Rev. A **83**, 033816 (2011).
- [18] A. M. Yao, New Journal of Physics **13**, 053048 (2011).
- [19] A. K. Jha, G. S. Agarwal, and R. W. Boyd, Phys. Rev. A **84**, 063847 (2011).
- [20] F. M. Miatto, H. D. L. Pires, S. M. Barnett, and M. P. van Exter, The European Physical Journal D **66**, 263 (2012).
- [21] Y. Zhang and F. S. Roux, Physical Review A **89**, 063802 (2014).
- [22] A. Mair, A. Vaziri, G. Weihs, and A. Zeilinger, Nature **412**, 313 (2001).
- [23] J. B. Pors, S. S. R. Oemrawsingh, A. Aiello, M. P. van Exter, E. R. Eliel, G. W. 't Hooft, and J. P. Woerdman, Phys. Rev. Lett. **101**, 120502 (2008).
- [24] A. K. Jha, J. Leach, B. Jack, S. Franke-Arnold, S. M. Barnett, R. W. Boyd, and M. J. Padgett, Phys. Rev. Lett. **104**, 010501 (2010).
- [25] W. H. Peeters, E. J. K. Verstegen, and M. P. van Exter, Phys. Rev. A **76**, 042302 (2007).
- [26] H. Di Lorenzo Pires, H. C. B. Florijn, and M. P. van Exter, Phys. Rev. Lett. **104**, 020505 (2010).
- [27] D. Giovannini, F. Miatto, J. Romero, S. Barnett, J. Woerdman, and M. Padgett, New Journal of Physics **14**, 073046 (2012).
- [28] G. Kulkarni, R. Sahu, O. S. Magaña-Loaiza, R. W. Boyd, and A. K. Jha, Nature communications **8**, 1054 (2017).
- [29] C. K. Hong and L. Mandel, Phys. Rev. A **31**, 2409 (1985).
- [30] S. P. Walborn, C. Monken, S. Pádua, and P. S. Ribeiro, Physics Reports **495**, 87 (2010).
- [31] D. Eimerl, L. Davis, S. Velsko, E. Graham, and A. Zalkin, Journal of applied physics **62**, 1968 (1987).